Temperature targets, deep uncertainty and extreme events in the design of optimal climate policy

Published Version:
Agliardi, E., Xepapadeas, A. (2022). Temperature targets, deep uncertainty and extreme events in the design of optimal climate policy. JOURNAL OF ECONOMIC DYNAMICS & CONTROL, 139, 1-19 [10.1016/j.jedc.2022.104425].

Availability:
This version is available at: https://hdl.handle.net/11585/888491 since: 2022-06-10

Published:

DOI: http://doi.org/10.1016/j.jedc.2022.104425

Agliardi, E., & Xepapadeas, A. (2022). Temperature targets, deep uncertainty and extreme events in the design of optimal climate policy. ***Journal of Economic Dynamics and Control*****,** ***139*****, 104425.**

The final published version is available online at:

https://doi.org/10.1016/j.jedc.2022.104425

Temperature Targets, Deep Uncertainty and Extreme Events in the Design of Optimal Climate Policy

Elettra Agliardi[1] and Anastasios Xepapadeas[2]
[1]University of Bologna
[2]Athens University of Economics and Business and University of Bologna

February 21, 2022

Abstract

We study optimal climate policy consistent with the constraint that average global temperature remains below 1.5°C relative to pre-industrial levels. We consider a holistic representation of uncertainty including traditional risk, deep uncertainty and stochastic arrivals of climate-related disasters. Using robust control methods, we derive optimal emission and carbon tax paths and calculate when temperature exceeds the target in the absence of the constraint. We show that policy under deep uncertainty requires strong action now relative to pure risk but the policy stringency is reversed later. Preliminary estimates suggest that the COVID-19 impact on attainment of the temperature target is negligible.

JEL Classification: Q54, D8

Keywords: temperature target; damage volatility; deep uncertainty; model misspecification; extreme events; robust control; emission scheduling; carbon taxes.

1 Introduction

In the Paris Agreement, adopted on 12 December 2015, 195 parties agreed to hold the increase in the global average temperature to well below 2°C above pre-industrial levels and to pursue efforts to limit the temperature increase – the temperature anomaly – to 1.5°C above pre-industrial levels, recognizing that this would significantly *"reduce the risks and impacts of climate change"* (Article 2 1.(a) of the Paris Agreement). Since then, several approaches have been proposed to estimate carbon budgets that are compatible with the specified temperature target. More research has been dedicated to estimates of the 2°C carbon budget (Wigley, 2004; Knutti *et al.*, 2005; Matthews *et al.*, 2009; Meinshausen *et al.*, 2009) than to the carbon budget associated with the more recently introduced 1.5°C temperature target (Matthews *et al.*, 2017; Mengis *et al.*, 2018). The 1.5°C is also the target of the European Green Deal (EGD), an initiative announced by the European Commission (2019) in December 2019. The central objective of the EGD is to attain a climate neutral EU by 2050, which means that the EU will aim to reach net-zero greenhouse gas (GHG) emissions by that year. Carbon neutrality by the EU is therefore in full alignment with the 1.5°C target.

However, the setting of a temperature target generates a number of issues regarding the optimal way of attaining the target and the associated policy instruments. Since there are substantial uncertainties in both climatic and economic conditions (Heal and Millner, 2014), an important question is how these uncertainties affect the attainment of the temperature target and the associated optimal policies.

Significant uncertainties associated with fundamental parameters of the climate, such as climate sensitivity, have been pointed out by Pindyck (2017). Furthermore, although there has been significant progress in estimating historical damages from climate change (e.g., Burke *et al.*, 2015), we know very little about the damage function, which is one of the most important building blocks of forward-looking optimizing climate-economy models.[1] Anthoff and Tol (2013) and Gillingham *et al.* (2016) characterize parameters of the climate–economy nexus, which embody considerable uncertainties, while Lemoine (2010), Nordhaus and Moffat (2017) and Hassler *et al.* (2018) discuss in detail the impacts of uncertainty on climate sensitivity. Typically, in these works uncertainty takes the form of risk, where objective or subjective probabilities are assigned to stochastic events. In climate change, however, uncertainty seems to be *"deeper"* than just risk.

[1] There is substantial discussion and – perhaps more importantly – uncertainty about the appropriate damage function, due to imperfect understanding of feedback effects, among other things (IPCC, 2014). Discussion of our limited knowledge of the damage function appears in Weitzman (2010) and Pindyck (2012, 2013, 2017).

Meinshausen *et al.* (2009), for example, present a set of densities associated with climate sensitivity which raises the issue of which one a planner or a regulator will choose to incorporate into the coupled model of economy and climate. Such a choice goes beyond choice under risk and enters the realm of deep uncertainty (Barnett *et al.*, 2020, 2021).

In a temperature-targeting model, it would be natural to associate "deep uncertainty" with temperature dynamics, since these dynamics are governed by parameters such as climate sensitivity of transient carbon response (TCRE), which characterize the link between GHG emissions, the evolution of the temperature anomaly and the economic damages it generates. Rudik (2020) develops a sophisticated economic model focusing on damage uncertainty within a robust control version of a DICE model and analyzes how the policy maker's concern for misspecification affects policy. His model, however, is not a temperature-targeting model and his damage function does not capture damages from the arrival of *"rare"* climate-related disasters which are caused by the increase in the temperature anomaly and might generate spikes in the smooth trend of the damage function. The impacts of extreme events have been emphasized by Pindyck (2012, 2013, 2017), and recent research stressed their importance in understanding the effects of climate change (e.g., Cai and Lontzek, 2019). Furthermore, since recent empirical results show that the number of climate-related disasters increases with the temperature anomaly (Karydas and Xepapadeas, 2019), their introduction will undoubtedly increase the realism of the damage function.

The COVID-19 pandemic shock and the related recession have added further types of uncertainty, which may influence the objective of carbon neutrality. According to a very recent International Energy Agency report (IEA, 2020), global CO_2 emissions were expected to decline during 2020 to 30.6 $GtCO_2$, which is 8.3% lower than in 2019 (36.8 $GtCO_2$) (Le Quére *et al.*, 2020). Given the realization of this shock and the predictions about the expected recovery of the world economy, a new question emerges: is the COVID-19 shock going to affect the attainment and the timing of the temperature target?

In this context, the contribution of our paper consists of: (i) exploring the impact of concerns about deep uncertainty in conjunction with the arrival of extreme events on the attainment of the temperature target and the associated policy; and (ii) providing a preliminary comparison between the pre- and post-COVID-19 predictions regarding the attainment of the temperature targets. Our paper provides, therefore, a conceptual framework and suggests climate policy by deriving emission pathways and carbon tax paths which attain a given temperature target optimally under conditions of deep uncertainty regarding temperature dynamics and climate change damages, arrival of rare climate disasters and exogenous shocks such as COVID-19.

Our conceptual framework is developed in the context of a robust control problem in the spirit of Hansen and Sargent (2001), where a welfare objective which includes a stochastic damage function is optimized under the temperature constraint that the change in global average temperature will never exceed a target, e.g., 1.5°C, relative to the pre-industrial period. As discussed in Anderson *et al.* (2014), even though this approach is not the only one for robustness analysis, it is convenient for analytical computations and appropriate for incorporating uncertainties related to temperature and damage dynamics. The temperature constraint formulation is based on the climate literature developed over the last decade (Matthews *et al.*, 2009, 2012) which links, through an approximately linear relationship, the temperature anomaly with cumulative carbon emissions. The damage function consists of a deterministic part, which is a quadratic function of past emissions, and a stochastic part, which is modelled by an arithmetic Brownian motion. The Brownian motion is distorted to introduce deep uncertainty and misspecification concerns. Furthermore, climate disasters are introduced by a jump process which follows a nonhomogeneous Poisson process, with the arrival rate of the disaster being an increasing function of temperature.

Our paper is close in spirit to the so-called "analytical integrated assessment models (IAMs)" (Traeger, 2015, 2018), which calculate welfare maximizing carbon emissions and optimal carbon prices based on simplified low-dimensional models that often yield closed-form solutions. Notable examples are Golosov *et al.* (2014), van den Bijgaart *et al.* (2016) and Gerlagh and Liski (2018). However, they are dynamic general economic equilibrium models, in contrast to our more parsimonious reduced-form approach. Our paper deals with temperature caps, as originally introduced by Nordhaus (1982), Tol (2013) and more recently van der Ploeg (2018), even though they are deterministic models. Temperature caps under uncertainty are studied in Olijslagers et al (2021) and Fitzpatrick and Kelly (2007). Olijslagers et al (2021) allow also for jump process risks with the intensity increasing in temperature, traditional risks for the growth of the economy and damage and study the impact of temperature caps on carbon pricing. Fitzpatrick and Kelly (2007) study a IAM with uncertainty about climate sensitivity, random weather shocks and Bayesian learning. They calculate the optimal emissions policy with and without probabilistic stabilization targets and compute the welfare costs of uncertainty in both cases. None of the papers listed above deal with "deep" uncertainty in the context of robust control models. To the best of our knowledge, our paper is the first to deal with deep uncertainty and temperature-targeting.

Our main contribution is that we provide a holistic representation of uncertainty in climate change by using a relatively simple model for deriving optimal climate policy which satisfies a given temperature target. Uncertainty is studied in the form of traditional risk, but also in the form of misspecification concerns, which affect the evolution of temperature and damages. Furthermore, we incorporate the arrival of environmental-related disasters which, in line with empirical observations, arrive more often as temperature increases. The optimal climate policy is obtained by the application of robust control methods. When this policy is compared with one that ignores concerns about deep uncertainty, a measure of the "insurance" that society should buy against worst case evolution of damages due to misspecification concerns or arrival of climate-related disasters emerges. We provide a measure of the "welfare cost" of this insurance.

Our calibrations suggest that with optimal unconstrained policies the estimated carbon budget consistent with the 1.5°C target is likely to be exhausted in less than 70 years, while optimal constrained paths attain the target with higher carbon taxes relative to the unconstrained case. Under deep uncertainty our results support the policy of "taking strong action now". Precautionary policy in the context of robust control is costly in terms of our welfare indicator. Finally, the COVID-19 shock seems to have negligible effects on the evolution of the temperature anomaly.

The rest of the paper is organized as follows. Section 2 describes the model. Section 3 presents the robust control problem, while Section 4 introduces the possibility of "rare" climate-related disasters. Section 5 introduces the pandemic shock, and Section 6 develops numerical simulations with calibrated data which allow us to evaluate when the 1.5°C target can be implemented and what the corresponding optimal carbon tax policy for the pre- and post-pandemic regimes is. Section 7 concludes. The proofs, the calibration and the code for the solution of the optimization problems appear in the Appendix.

2 The model

We consider the problem of a social planner/regulator who seeks to maximize global wellbeing within a fixed time horizon by choosing paths for GHG emissions subject to the constraint that, within the time horizon, temperature will not exceed a given level relative to the pre-industrial period. The social planner faces two sources of uncertainty: uncertainty about damages from climate change and uncertainty about the evolution of temperature. The social planner is also concerned about deep uncertainty and possible misspecification of the damage function and temperature dynamics. We solve the planner's problem by adopting a dynamic optimization framework which uses the methods of robust control developed by Hansen and Sargent (e.g., Hansen *et al.*, 2006, Hansen and Sargent, 2008).

A decision maker characterized by robust preferences takes into account the possibility that the model used to design policy, call it benchmark or approximating model P, may not be the correct one but only an approximation of the correct one. Other possible models different from the benchmark, say $Q_1, ..., Q_J$, which surround P, should also be taken into account with the relative differences or distance among these models measured by an entropy measure. The benchmark model P and the approximate models can be regarded contained in an entropy ball (Hansen and Sargent, 2008). The radius of this ball determines the maximum misspecification that the decision maker is willing to accept. Hansen and Sargent (2003) characterize robust control as a theory "... [that] instructs decision makers to investigate the fragility of decision rules by conducting worst-case analyses," and suggest that this type of model uncertainty can be related to ambiguity or deep uncertainty and interpreted as the decision maker's response to "Knightian uncertainty" and a recursive version of maxmin expected utility theory. The models inside the entropy ball are close enough to the benchmark model so that they are difficult to distinguish with finite data sets. Then robust decisions rules are obtained by introducing a fictitious " adversarial agent" which we will refer to as "Nature". Nature promotes robust decision rules by forcing the regulator, who seeks to maximize (minimize) an objective, to explore the fragility of decision rules with regard to departures from the benchmark model. A robust policy means that lower bounds to the policy's performance are determined by Nature – the adversarial agent – which acts as a minimizing (maximizing) agent when constructing these lower bounds. In the context of our model the regulator is concerned about misspecfications in the damage function and temperature dynamics and is forced the consider policies when he/she is concerned about misspecifications of the benchmark models.

Robust preferences and the concept of a fictitious adversarial agent is one approach to decision making under uncertainty. Cerreia-Vioglio et al. (2011) introduced a general class of complete and transitive preferences that are monotone and convex, which they call "uncertainty-averse" preferences. These preferences include as special cases the seminal Gilboa-Schmeidler minimax utility model (Gilboa and Schmeidler 1989) and its extension to dynamic robust control by Hansen and Sargent; the variational preferences model (Maccheroni et al. 2006); the smooth ambiguity model of Klibanoff et al. (2005); and the Petrakou et al. (2021) ambiguity averse Frechet mean preferences. These models do not include the concept of the adversarial agent, but are less tractable, compared to the robust control models, in the dynamic context which is necessary for a meaningful analysis of climate policies.

2.1 The damage function and misspecification concerns

In this section we introduce the damage function. Our specification of the damage function captures three main features, that is, the (deterministic) dependence on cumulative emissions, its stochastic fluctuations and the concerns of the regulator regarding possible misspecifications of the damage function.

We adopt a discrete time schedule, where $1, 2, ..., N$ denote the times at which the decisions on the production process are made by observing the information available at the current time. In the sequel, expectations conditional on the information available at time k will be denoted as E_k. Let x_1,...,x_N denote the amount of GHG emissions at time $1, 2, ..., N$ as a consequence of the production process.

The total damage due to GHG emissions is described by a stochastic process D_t. We assume that the benchmark model of damage consists of two components. The first component, D_t^0, which is related to the global warming potential of GHGs, allows us to describe fluctuations in actual economic damages around its deterministic component in a random way. A simple model for these random fluctuations is an arithmetic Brownian motion, i.e., $dD_t^0 = \sigma dW_t$, where W_t is a Wiener process with respect to the fixed filtration that represents the information available to the decision maker.[2]

The second component of damage is deterministic. We specify the damage function as a function of emissions (as also in Nordhaus, 2007, and van der Ploeg, 2014), whereas other models express damages as a function of a climate indicator, such as global temperature (see, e.g., Weitzman, 2010). In Section 2.3 we show that the deterministic part of our damage function is consistent with a quadratic damage function specification when the evolution of the temperature anomaly is a mapping from cumulative emissions into changes in the global mean temperature, as outlined in Matthews et al (2009).

We assume that the incremental damage, that is the extra damage from an extra unit of emissions, is $\Delta D_k = \varepsilon x_k \sum_{j=1}^{k-1} e^{-\rho(k-j)} x_j$, $\varepsilon > 0$. Therefore, we adopt a non-linear impact of the emissions on damages, which is consistent with the literature showing strong carbon/climate feedbacks and more persistent warming due to GHGs (see, e.g., Solomon *et al.*, 2010). Furthermore, damages from GHG emissions could be gradually dissipated and thus their negative economic impact could become weaker with the passage of time. This is because some of the damaging GHGs have shorter permanence time in the atmosphere than CO_2. Methane (CH_4) emissions, for example, have a medium-term permanence of 12 years on average in the atmosphere, and thus they will cease to create damages after the period of permanence is exceeded. Here $\rho \geq 0$ denotes the parameter governing this weakening of damages associated with past emissions. In other words, when $\rho = 0$, the negative effect of emissions persists forever, while for $\rho > 0$, neg-

[2]More generally, this assumption can be replaced by any martingale with respect to the reference filtration. Here we adopt an arithmetic Brownian motion because it is the easiest way to model randomness and allows us to obtain an explicit analytic solution. The occurrence of negative damage due to the assumption of an arithmetic Brownian motion is avoided by taking small values of the volatility σ. Questions of uncertainty with non-Gaussian distributions on various variables have recently been explored in van den Bremen and van der Ploeg (2018).

ative effects weaken with passage of time and at the extreme case of $\rho = \infty$, there is immediate dissipation of damages.

Arguing recursively, the total cumulated damage, soon after time k, takes the form:

$$\sum_{j=1}^{k} x_j D_j^0 + \varepsilon \sum_{j=1}^{k} \left(\frac{x_j^2}{2} + \sum_{i<j} e^{-\rho(j-i)} x_i x_j \right) \tag{1}$$

where D^0 is the stochastic component which follows an arithmetic Brownian motion with zero drift and variance parameter σ^2.

Therefore, the total cumulated damage is characterized by a non-linear effect of past emissions and the interactions among past emissions emitted at different points of time in the past. This non-linear feature captures the exceptional persistence displayed by CO_2, which renders its warming nearly irreversible for more than 1,000 years, and also by other GHGs which – although not irreversible – persist notably longer than the anthropogenic changes in the GHGs' concentrations themselves (see Solomon *et al.*, 2010).

Figure 1 plots a path for the total cumulated damage after two subsequent emissions. In panel (a) damages from past emissions are reduced with the passage of time, $\rho > 0$, while in panel (b) the damage impact of past emissions remains the same, $\rho = 0$.[3]

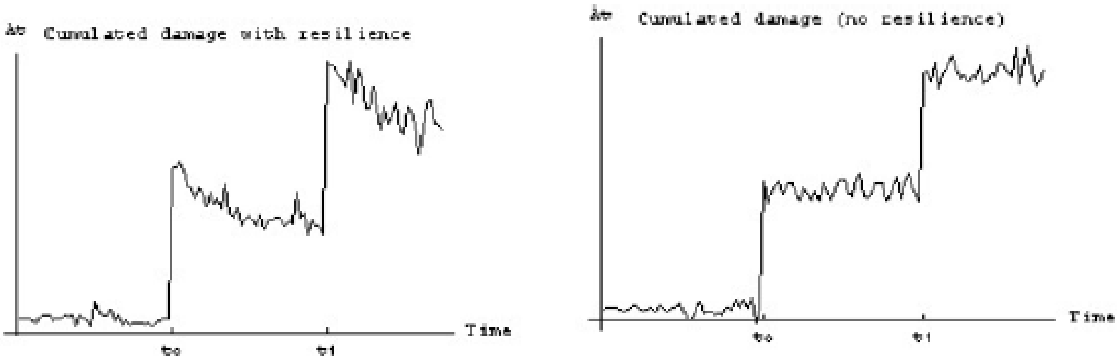

(a) Case $\rho = 0.1$ (b) Case $\rho = 0$

Figure 1. Cumulated damages with two subsequent emissions

[3] As shown in section 2.3 for $\rho = 0$ the deterministic part of (1) is consistent with a quadratic damage function in the temperature anomaly, when the dynamics of temperature dynamics are governed by the approximately linear relationship between the temperature anomaly and cumulative carbon emissions.

We assume that expression (1) represents a benchmark case for the damage function for the regulator. The regulator, however, is concerned about possible misspecification of the damage function. These concerns can be introduced by allowing additive distortions in (1), which accumulate like $\sqrt{e}\sigma_0 (\eta_t + z_t)$, where σ_0 is volatility, e is a small noise parameter, z_t is i.i.d. and η is the distortion in the damage function. The distortion reflects possible misspecifications relative to the benchmark model which corresponds to $\eta = 0$. Misspecification could be responsible for additional damages, $\sum_{j=1}^{k} \sqrt{e}\sigma_0 (\eta_j + zj)$. If we consider a multiplier robust control problem (e.g., Hansen *et al.*, 2006), the penalty associated with the distortion relative to the benchmark model can be expressed as $\frac{\eta_t^2}{2\theta(e)}$, where $\theta(e)$ is the robustness parameter.

It has been shown (Campi and James, 1996) that if $\theta(e) = \theta_0 e$, then as $e \to 0$, the stochastic robust control problem is reduced to a simpler "deterministic robust control problem" and in our case the distorted damage function can be written as:

$$\sum_{j=1}^{k} x_j D_j^0 + \varepsilon \sum_{j=1}^{k} \left(\frac{x_j^2}{2} + \sum_{i<j} e^{-\rho(j-i)} x_i x_j \right) + \sum_{j=1}^{k} \sigma_0 \eta_j x_j. \tag{2}$$

Therefore, the damage function (2) consists of three parts. The first is a purely stochastic component, the second is a deterministic component, while the third reflects potential distortions of the benchmark model which consists of the first two components. These distortions are associated with the fact that a regulator is concerned about misspecifications of the benchmark model which might imply additional damages. The regulator cannot, however, resolve these concerns using existing data and should therefore address them when designing climate policy. This is the reason for applying robust control methods.

2.2 The regulator's objective function

The objective of the regulator is to maximize wellbeing net of the expected total damage over a time horizon N, given potential temperature targets. Here we adopt robust control theory to capture the idea that the regulator doubts his/her model. As Hansen et al. (2006) show, different alternative mathematical formulations can be used, which have in common i) the idea of representing the decision-maker's benchmark model with a cloud of models that are difficult to distinguish with finite data - and are formed perturbing the benchmark model; ii) adding a malevolent second agent that can alter the stochastic process and plays a penalty game. Deviating from the benchmark model is penalized since the regulator does not choose the 'best estimate' model. The size of the penalty represents the distance between an alternative model and the reference model. In the multiplier robust control setting, we get a zero-sum, two-player game, in which the maximizing player (the social planner/regulator) chooses a best response to a adversriat agent ("Nature") that can alter the stochastic process within prescribed limits by choosing a distortion η which will "harm" the planner's objective. We solve below for the optimal choices made by both the maximizing agent and the minimizing agent.[4] We will also study the case of a regulatory target in terms of temperature, and thus cumulative emissions, which is set by international agreements within the time horizon.

In this paper a quadratic utility will be adopted, that is, $U(x) = ux - \frac{1}{2}wx^2$, which is common in the literature (e.g., Dockner and Van Long, 1993; Karp and Zhang, 2006; Manoussi et al., 2018). This function links gross wellbeing with emissions and could be seen as a reduced form of a problem where utility is a function of consumption, which itself depends on economic output that, in turn, is a function of emissions.[5] The parameter u measures the effect on marginal benefits from emissions, while w the strength

[4] We refer to Hansen *et al* (2006) for the equivalence between the formulations in terms of (i) risk-sensitive control problem; (ii) penalty robust control problem; (iii) constraint robust control problem. Hansen *et al.* (2006) discuss different concepts of equilibrium used in the robustness approach, because these types of zero-sum games may differ in various dimensions (the protocols that govern the timing of players' decisions; the constraints on the malevolent player's choices; the mathematical spaces in terms of which the games are posed). However, they showed that all the formulations give rise to identical decision processes in linear quadratic settings.

[5] Picture a simple growth model with the utility function $U(c) = ac - \frac{1}{2}bc^2$, where c denotes consumption. Let us define the budget constraint for the economy with an Ak production function such as $c_t = Ak_t - k_{t+1} + (1-d)k_t$, where k is the capital stock and d is the depreciation rate. If we define emissions as proportional to output, that is $x_t = sAk_t$, where s is an exogenous parameter of emission intensities, then we get the following expression for the the utility function: $U(x_t) = a(\frac{x_t}{s} - \frac{x_{t+1}}{sA} + (1-d)\frac{x_t}{sA}) - \frac{1}{2}b(\frac{x_t}{s} - \frac{x_{t+1}}{sA} + (1-d)\frac{x_t}{sA})^2$, and therefore the sum of the utility functions over t is: $\sum_t U(x_t) = a\sum_t(\frac{x_t}{s} - \frac{x_{t+1}}{sA} + (1-d)\frac{x_t}{sA}) - \frac{1}{2}b\sum_t(\frac{x_t}{s} - \frac{x_{t+1}}{sA} + (1-d)\frac{x_t}{sA})^2$. If $b = 0$, then $\sum_t U(x_t) = \frac{a}{s}(1 - \frac{d}{A})\sum_t x_t = u\sum_t x_t$. Therefore, if utility is also linear in consumption, then it becomes a function of emissions too. This argument can be applied to the general case of a quadratic utility function whenever w is small.

of their diminishing returns. The choice of a quadratic utility function is also motivated by the invariance result to timing protocols provided by Hansen et al. (2006), which implies a form of dynamic consistency. We allow for discounting, where the discount factor – reflecting the net benefit discount rate – is set equal to δ, $\delta \in (0,1)$. Thus, the objective function to be extremized is of the form:

$$\mathbb{E}_0\left[\textstyle\sum_{k=1}^{N}\delta^k\left(ux_k-\frac{1}{2}wx_k^2-x_kD_k^0-\varepsilon\left(\frac{x_k^2}{2}+\displaystyle\sum_{i<k}e^{-\rho(k-j)}x_ix_k\right)-\sigma_0\eta_kx_k+\frac{\eta_k^2}{2\theta}\right)\right], \tag{3}$$

where the minimizing agent ("Nature") chooses $\{\eta_k, k=1,...,N\}$ at date 0, committing to it until the end, and the maximizing agent (the social planner/regulator) then chooses $\{x_k, k=1,...,N\}$. Problem (3), in Hansen and Sargent's terminology is the *multiplier robust control problem* which is associated with a *constrained control problem* in which the entropy distance between the benchmark model and the approximate models does not exceed an upper bound. The parameter θ is a *preference-for-robustness parameter*.[6] When $\theta \to 0$ there are no concerns about model misspecification and the benchmark model which describes that decision problem under risk is the relevant problem for policy design. As θ increases misspecification concerns are taken into account and robust policy rules should be formulated.

Note that the expectation of the cumulated effect of emissions can be rewritten as:

$$\mathbb{E}_0\left[\sum_{k=1}^{N}x_kD_k^0+\varepsilon\sum_{k=1}^{N}\left(\frac{x_k^2}{2}+\sum_{i<k}e^{-\rho(k-i)}x_ix_k\right)+\sum_{k=1}^{N}\sigma_0\eta_kx_k\right]=$$
$$D_0\textstyle\sum_{k=1}^{N}x_k+\varepsilon\sum_{k=1}^{N}\left(x_kV_{k-1}+\frac{x_k^2}{2}\right)+\displaystyle\sum_{k=1}^{N}\sigma_0\eta_kx_k,$$

where $V_k=\sum_{j=1}^{k}e^{-\rho(k+1-j)}x_j$ for $k\geq 1$ (and $V_0=0$) is the volume of cumulated emissions (up to time $k+1$).

If the regulator is also concerned about the risk of random fluctuations in damage, then an additional term in the form of a variance should be added,

[6] It can be shown (Hansen and Sargent 2001) that under certain conditions θ is the Langrangean multiplier associated with the entropy constraint of the constrained control problem.

so the objective function to be extremized takes the form:

$$\mathbb{E}_0 \sum_{k=1}^N \delta^k \left[(u - D_0)x_k - \left(\frac{(\varepsilon + w)x_k^2}{2} + \varepsilon x_k V_{k-1} \right) - \sigma_0 \eta_k x_k + \frac{\eta_k^2}{2\theta} \right]$$

$$-\frac{\gamma}{2} \mathrm{var}_0 \left[\sum_{k=1}^N \delta^k x_k D_k^0 + \varepsilon \sum_{k=1}^N \delta^k \left(\frac{x_k^2}{2} + \sum_{i<k} e^{-\rho(k-i)} x_i x_k \right) + \sum_{k=1}^N \delta^k \sigma_0 \eta_k x_k \right],$$

where γ denotes the risk aversion parameter. The parameter γ embodies the concern of the regulator regarding the uncontrolled effect of the outstanding volume of emissions, measured by the variance. Note that the introduction of a variance term has not been widely explored in the literature, while it is relevant to study the effects of the variability of system behavior changes.[7] Our formulation can be justified in the framework of the standard mean-variance approach, which has been employed extensively in financial economics. It implies that if the regulator is also adverse to risk, then he/she will solve a constrained maximization problem, that is maximize expected wellbeing net of total damage subject to the constraint that risk (i.e., variance of the objective function) is not too big. Observe that the variance term can be written as:

$$\mathbb{E}_0 \left[\sigma^2 \left(\sum_{k=1}^N x_k W_k \right)^2 \right] = \sigma^2 \sum_{k=1}^N \left[x_k^2 k + 2x_k \sum_{i<k} x_i i \right].$$

The variance term introduces risk as traditional risk (risk intrinsic to damage). The robustness parameters introduce uncertainty as misspecification of the benchmark model, that is, concerns of the social planner about the "true" model. Therefore, they complement each other.

In the following, we confine ourselves to the case of equally-spaced time intervals Δt to simplify the exposition. Furthermore, we set $e^{-\rho\Delta t} = \beta$ and $\gamma\sigma^2\Delta t = \Gamma$. Thus, the unconstrained extremization problem – and the

[7] See Brock and Carpenter (2006) who stress that increased variance may provide a leading indicator of regime shifts that can be used in ecosystem management.

corresponding robust control problem – can be defined as:

$$\sup_{\{x_k\}} \inf_{\{\eta_k\}} \sum_{k=1}^{N} \delta^k \left[(u - D_0)x_k - \left((\varepsilon + w + \Gamma k)\frac{x_k^2}{2} + \varepsilon x_k \sum_{j=1}^{k-1} \beta^{k-j} x_j \ + \right.\right.$$
$$\left.\left. \Gamma x_k \sum_{i<k} i x_i + \sigma_0 \eta_k x_k \right) + \frac{\eta_k^2}{2\theta} \right].$$

2.3 The temperature constraint and misspecification concerns

Our objective is to study how the optimal scheduling of emissions is affected by temperature targets that have to be achieved at specified dates, as stated in the monitoring procedures of the international climate change agreements. The goal of avoiding more than 1.5°C increase in warming relative to the pre-industrial period was the agreed-upon target at the UN climate-change meeting in Paris in 2015. This is consistent with the use of the cumulated carbon budget which should not be exceeded for a given threshold temperature, as formulated by Matthews *et al.* (2009), Matthews *et al.* (2012) and, more recently, in the IPCC (2018) special report.

Assume that we are at time $k = 1$ and the regulator sets an upper threshold on temperature change (relative to pre-industrial time) which should not exceed, say, α°C (e.g., 1.5°C) within the horizon $[1, N]$. We know from Matthews *et al.* (2009) that for the period $[1, N]$ the change in temperature will be

$$\Delta\Upsilon_N = \Upsilon_N - \Upsilon_1 = \Lambda \textstyle\sum_{k=1}^{N} x_k, \tag{4}$$

where Λ denotes the TCRE parameter.

Note that the deterministic part of the damage function (2) is consistent with a quadratic damage function specification when the evolution of the temperature anomaly is characterized by (4) for $\rho = 0$. In this case a quadratic damage function in terms of the anomaly can be defined as

$$D(\Delta\Upsilon_N) = \omega\,(\Delta\Upsilon_N)^2 = \omega\left(\Lambda \textstyle\sum_{k=1}^{N} x_k\right)^2, \tag{5}$$

and the damage function (5) corresponds to the deterministic part of (2) for $\rho = 0$ and appropriate readjustments of the parameters. In the numerical simulations section of this paper we discuss the sensitivity of the solutions to $\rho \geq 0$.

Since our temperature constraint is $\Delta \Upsilon_N \leq \alpha$, we have

$$\Lambda \textstyle\sum_{k=1}^{N} x_k \leq \alpha. \tag{6}$$

Assume that the social planner has misspecification concerns about temperature dynamics (6) and the distortions associated with these concerns accumulate as $\sqrt{e}\sigma_m (h_t + z_t)$ where σ_m is volatility, e is a small noise parameter, z_t is i.i.d. and h is the distortion in the TCRE parameter. The distortion reflects possible misspecifications relative to the benchmark model (4) which corresponds to $h = 0$. Note that in this case $\sqrt{e}\sigma_m z_t$ represents traditional risk. Following the same argument as in the previous section, and letting $e \to 0$ where the penalty is of the form $\frac{h_t^2}{2\upsilon(e)}$, the temperature constraint becomes:

$$\Lambda \textstyle\sum_{k=1}^{N} x_k + \sum_{k=1}^{N} \sigma_m h_k \leq \alpha. \tag{7}$$

3 The robust control problem

With misspecification concerns about damages and temperature dynamics, the minimizing agent chooses distortions η and h to harm the planner's objective and the robust control problem becomes:

$$\begin{aligned} \sup_{\{x_k\}} \inf_{\{\eta_k, h_k\}} \sum_{k=1}^{N} \delta^k \Bigg\{ (u - D_0)x_k - \Bigg[(\varepsilon + w + \Gamma k)\frac{x_k^2}{2} + \varepsilon x_k \sum_{j=1}^{k-1} \beta^{k-j} x_j \\ + \Gamma x_k \sum_{i<k} i x_i + \sigma_0 \eta_k x_k \Bigg] + \frac{\eta_k^2}{2\theta} + \frac{h_k^2}{2\upsilon} \Bigg\}, \text{ subject to (7).} \end{aligned} \tag{8}$$

The higher θ and υ are, the more the regulator is concerned about misspecification regarding the damage function and the accuracy of the budget constraint which reflects temperature dynamics. Thus the social planner chooses x_k and Nature, which is the adversarial agent, chooses η_k and h_k, with the robustness parameter υ having the same interpretation as θ. A similar optimization applies to the unconstrained – regarding the temperature target – problem.

The constrained optimization problem can be solved through the Kuhn-

Tucker method,

$$\mathfrak{L}(x_1,...,x_N,\lambda) = \tag{9}$$
$$\sum_{k=1}^{N}\delta^k\left\{(u-D_0)x_k - \left[(\varepsilon+w+\Gamma k)\frac{x_k^2}{2}+\varepsilon x_k\sum_{j=1}^{k-1}\beta^{k-j}x_j+\Gamma x_k\sum_{i<k}ix_i+\sigma_0\eta_k x_k\right]\right.$$
$$\left.+\frac{\eta_k^2}{2\theta}+\frac{h_k^2}{2\upsilon}\right\}-\lambda\left[\Lambda\sum_{k=1}^{N}x_k+\sum_{k=1}^{N}\sigma_m h_k-\alpha\right],$$

where $\mathfrak{L}$ is the Lagrangean and $\lambda \geq 0$ is a Lagrangian multiplier. Then the first-order conditions for the choices made by both the maximizing agent and the minimizing agent are $\frac{\partial\mathfrak{L}}{\partial x_k}=0$, $\frac{\partial\mathfrak{L}}{\partial\eta_k}=0$ and $\frac{\partial\mathfrak{L}}{\partial h_k}=0$, $k=1,...,N$. The optimal emission policy is determined by solving a linear system of the form:

$$M\begin{pmatrix} x_1 \\ ... \\ x_N \end{pmatrix} = \begin{pmatrix} (u-D_0)-\lambda\Lambda\delta^{-1} \\ ... \\ (u-D_0)-\lambda\Lambda\delta^{-N} \end{pmatrix} \tag{10}$$

$$M = \begin{pmatrix} (\varepsilon+w+\Gamma+\sigma_o^2\theta) & (\varepsilon\beta+\Gamma) & ... & (\varepsilon\beta^{N-1}+\Gamma) \\ (\varepsilon\beta+\Gamma) & (\varepsilon+w+2\Gamma+\sigma_o^2\theta) & ... & (\varepsilon\beta^{N-2}+2\Gamma) \\ ... & & & ... \\ (\varepsilon\beta^{N-1}+\Gamma) & (\varepsilon\beta^{N-2}+2\Gamma) & ... & (\varepsilon+w+N\Gamma+\sigma_o^2\theta) \end{pmatrix}. \tag{11}$$

Proposition 1 provides the solution to our optimization problem.

Proposition 1 *Assume that $u > D_0$ and that an upper threshold, $\alpha^\circ C$, is set by the regulator on temperature change (relative to pre-industrial time). Then the optimal policy is obtained as:*

$$\mathbf{x}^* = \begin{pmatrix} x_1^* \\ ... \\ x_N^* \end{pmatrix} = M^{-1}\begin{pmatrix} (u-D_0)-\lambda\Lambda\delta^{-1} \\ ... \\ (u-D_0)-\lambda\Lambda\delta^{-N} \end{pmatrix},$$

where the matrix M is defined in (11), and

$$\begin{aligned} \lambda &= \frac{(u-D_0)\Lambda\sum_{i,j}\widetilde{m}_{i,j}-\alpha}{\Lambda^2\sum_{i,j}\widetilde{m}_{i,j}\delta^{-j}-A} \\ \textit{with } A &= \sigma_m^2\upsilon\sum_i\delta^{-i} \textit{ and } M^{-1}=(\widetilde{m}_{i,j}). \end{aligned}$$

For the proof, see Appendix 1.

For a large time horizon, e.g. $N = 100$, the optimal path can be calculated through numerical methods which will be performed in Section 6. Observe that, by the envelope theorem, the Lagrangean multiplier λ in Proposition 1 is $\lambda = \frac{\partial V}{\partial \alpha}$ where V is the value function of the planner. Thus λ expresses the change in the optimized net global wellbeing from a small change in the temperature target.

3.1 The optimal carbon tax

Proposition 1 can be used to derive the optimal carbon tax both for the case where the temperature constraint is binding and for the unconstrained case. The optimal carbon tax can be computed solving for the tax rate at which the representative firm's profit-maximizing emissions equal the optimal emissions chosen by the regulator, as defined in Proposition 1. The representative firm faces an exogenous tax τ on emissions and solves a static problem

$$\max_{x_k} ux_k - \frac{1}{2}wx_k^2 - \tau_k x_k \ , \ k = 1, ...N,$$

which means that regulated emissions are:

$$x_k^0 = \frac{u - \tau_k}{w}.$$

The optimal tax should be chosen so that the firm's profit-maximizing emissions are equal to the optimal emissions chosen by the regulator. This means that

$$\frac{u - \tau_k}{w} = M^{-1}\left[(u - D_0)\Xi - \lambda\Lambda \begin{pmatrix} \delta^{-1} \\ ... \\ \delta^{-N} \end{pmatrix}\right],$$

where Ξ denotes an $N \times 1$ vector with all entries equal to 1. Solving for τ_k, we obtain

$$\tau_k = u - wM^{-1}\left[(u - D_0)\Xi - \lambda\Lambda \begin{pmatrix} \delta^{-1} \\ ... \\ \delta^{-N} \end{pmatrix}\right], \text{ or}$$

$$\tau_k = u - wx_k^* \ , \ k = 1, ...N, \tag{12}$$

where x_k^* are optimal emissions chosen by the regulator. Thus taxes are increasing over time if the optimal emission schedule is declining.

Proposition 1 can also be used to explore the unconstrained problem in which $\lambda = 0$ and optimal emissions are determined as:

$$\mathbf{x}^* = \begin{pmatrix} x_1^* \\ \ldots \\ x_N^* \end{pmatrix} = (u - D_0)M^{-1}\Xi. \tag{13}$$

Then, it is easy to determine whether and when the cumulative emissions of the optimal unconstrained schedule will lead to a temperature anomaly violating the temperature target, by plugging the unconstrained emission path into the temperature dynamics. Furthermore, the impact of changes in misspecification concerns on the optimal emission paths can be obtained through comparative analysis focusing on $\partial x_k^*/\partial\theta$, and $\partial x_k^*/\partial\eta$.

3.2 The welfare cost of robust control

Introducing concerns for misspecification and non-zero robustness parameters implies that there will be deviations between the optimal emission paths with misspecification concerns (C) and without misspecification concerns (NC), x_{kC}^*, x_{kNC}^* respectively. Thus the C paths correspond to decison making under uncertainty, while the NC paths rorresponding to t decision making under A question which arises in this case is whether, when a robust climate policy is pursued, the policy generates additional welfare costs or benefits relative to the case in which no misspecification concerns are involved.[8] To obtain an approximation of these additional welfare costs or benefits, we consider the global welfare indicator:

$$\begin{aligned} V^R \;=\; & \sum_{k=1}^{N} \delta^k \left\{ (u - D_0)x_{kR}^* - \left[(\varepsilon + w + \Gamma k)\frac{(x_{kR}^*)^2}{2} + \varepsilon x_{kR}^* \sum_{j=1}^{k-1} \beta^{k-j} x_{jR}^* + \right.\right. \\ & \left.\left. \Gamma x_{kR}^* \sum_{i<k} i x_i + \sigma_0 \eta_k^* x_{kR}^* \right] \right\} , R = C, NC. \end{aligned} \tag{14}$$

[8] We use the welfare indicator as if we were treating our Pareto optimal planner as a Pareto optimal Bayesian planner choosing an optimal solution under the worst case distribution.

Note that the welfare indicator does not include the penalty terms $\left(\frac{\eta_k^{*2}}{2\theta}, \frac{h_k^{*2}}{2\upsilon}\right)$ imposed by the minimizing agent, since they are in a sense fictitious and are used to determine the robust emission paths. The welfare indicator for the C case includes, however, the robust emission paths since the comparison is between the welfare corresponding to the NC and C states. Then the impact of taking into account misspecification concerns on wellbeing can be obtained by calculating

$$V^{NC} - V^{C}. \tag{15}$$

Since robust control and its link with a worst case scenario can be regarded as a precautionary policy, the difference $V^{NC} - V^{C}$, if positive, can be interpreted as the cost of been precautious. An estimate of the cost of robustness (or precaution) is presented in Section 6.1, where various penalty parameters are considered.

4 Adding the risk of climate-related disasters

Our model can be extended to the case of climate-related disasters. These are events that have possibly large negative impacts on the economy, occur very rarely and take place abruptly. Since the nature of risk of climate disasters is different from "normal" risk, as captured by a diffusion term, we assume that rising global temperature exposes the economy to risks of disasters which are modelled through jump processes. We explicitly take into account that it is hard to estimate the probability of a disaster and its expected impact by assuming that the regulator does not know the exact probability distributions of the arrival rate and the size of climate shocks. Earlier works studying disasters in a macroeconomic context (e.g., Barro, 2009) have been extended to include time-varying disaster probabilities and multi-period (i.e., persistent) disasters (e.g., Wachter, 2013) and climate-related disasters (Karydas and Xepapadeas, 2019). However, unlike this literature, we study the impact of jump risks on the optimal constrained emission paths.

In order to incorporate climate-induced disasters, we modify the stochastic process and add a jump process J_t, with upward jumps following nonhomogeneous Poisson processes whose intensity depends on temperature and thus on cumulated emissions. More specifically, we assume that the arrival rate q of an environmental disaster depends linearly on the temperature anomaly $\Delta\Upsilon$. That is,

$$q_k = q_0 + \xi \Delta\Upsilon_{k-1} \ , \ k = 1, ..., N \ , \tag{16}$$

which can be written as a function of cumulated emissions, as in Section 2.3, so that

$$q_k = q_0 + \xi \left[\Lambda \textstyle\sum_{j=1}^{k-1} x_j + \sum_{j=1}^{k-1} \sigma_m h_j \right] , \tag{17}$$

where Λ denotes the TCRE parameter. The size of jumps is related to the expected disaster damages. They are assumed to be proportional to a linearized representation of the benefit function, hence a function of emissions, i.e., $\zeta(a + bx_k)$. We assume independence between the processes W_t and J_t.

Following the same procedure as before, we can obtain an extension of Proposition 1 when the risk of extreme events is included. Thus, the optimal emission policy is obtained as:

$$\mathbf{x}^* = \begin{pmatrix} x*_1 \\ x*_2 \\ ... \\ x*_N \end{pmatrix} = \widehat{M}^{-1} \begin{pmatrix} (u - D_0 - q_0\zeta b - \lambda\Lambda\delta^{-1}) \\ (u - D_0 - q_0\zeta b - \xi\zeta b\lambda v\sigma_m^2\delta^{-1} - \lambda\Lambda\delta^{-2}) \\ ... \\ (u - D_0 - q_0\zeta b - \xi\zeta b\lambda v\sigma_m^2 \sum_{i=1}^{N-1}\delta^{-i} - \lambda\Lambda\delta^{-N}) \end{pmatrix} .$$

Following the same argument as in Section 3.1, we can also compute the optimal carbon tax in the case of extension to climate-related disasters, by replacing the new optimal emissions $\mathbf{x}^*$ chosen by the regulator in expression (14). The analysis regarding the welfare cost or robust control can easily be extended to include climate-related disasters.

5 The impact of the COVID-19 shock

The COVID-19 pandemic led to recession due to containment measures. Predictions from the IMF (2020) – which of course carry a large degree of uncertainty, or even "deep" uncertainty – indicate, for example, that relative to October 2019 the proportional change in world output is -6.4%. Furthermore, as recalled in our introduction, a sharp reduction in CO_2 emissions was reported during 2020. Here we are interested in incorporating the shock into our modeling and comparing pre- and post-pandemic optimal paths and carbon taxes.

We model the shock induced by the COVID-19 pandemic as a perturbation which shifts the utility function $U_k = \left(ux_k - \frac{1}{2}wx_k^2\right)$ downwards in the first i years of our planning horizon, assuming that this horizon starts now. The shift of the utility function U_k is modelled by a term $\Phi_i = 1 - (1 - \overline{\Phi})\left(\frac{1}{(1+H)^i}\right)$ in which $\overline{\Phi}$ and H are calibrated such that the drop in the first year of the benefit is equal to the IMF prediction and the recovery takes place within $\bar{R}$ years, that is, $i = 1, 2, ..., \bar{R}$, while for $k > \bar{R}$ the $\frac{1}{(1+H)^k}$ approaches zero to indicate that the COVID-19 initial shock does not affect the economy anymore. Thus the within-pandemic gross benefit function becomes $\Phi_i U_k$. The shift of the benefit function induces, in the context of the optimization model, an *"optimal emission reduction"* for $k = 1, 2, ...$ In order to start the optimization from the current level of emissions, we incorporate an exogenous shock which will restrict the initial optimal emission path at the current within-pandemic values. In our simulations we compare the post-pandemic emission paths with the pre-pandemic emission paths which corresponds to $\overline{\Phi} = 1$.

6 Numerical simulations

In this section we perform a numerical simulation with calibrated data. We solve the optimization problem with the Langrangian function (21) for a time horizon of 100 years. The calibration is described in Appendix 3.[9] We examine four possible scenarios coded 1,2,3,4 in Figures 2 and 3.

In scenario 1 there is no concern about model misspecification, that is, $\theta = \upsilon = 0$, and no impact from climate-related disasters, i.e., $\zeta = 0$. There is only risk associated with the *"traditional"* stochastic component of the damage function $dD_t^0 = \sigma dW_t$, with $\sigma > 0$. Thus, scenario 1 can be regarded as the benchmark model corresponding to decision making under risk. In scenario 2 we allow for impacts from climate-related disasters in the benchmark model, so $\zeta > 0$. In scenario 3 we introduce misspecification concerns in the damage function and the temperature dynamics, along with the possibility of climate-related disasters. In this case, $(\,(\theta, \upsilon)|\,\text{scenario 3}) > (0, 0)$. In scenario 4 we increase the misspecification parameters θ, υ relative

[9] Mathematica 12.0 was used for the solution of the optimization problem. The code is presented in the supplementary material.

to scenario 3 in order to examine the impact of increasing ambiguity on optimal paths. In this case, $((\theta, \upsilon)|\,\text{scenario 4}) > ((\theta, \upsilon)|\,\text{scenario 3})$.

The robustness parameters (θ, υ) are free parameters reflecting the misspecification concerns of the decision maker. Anderson et al. (2003), Hansen and Sargent (2008)[10] use detection error probabilities to quantify the robustness parameters. The approach is to set the robustness parameter so that, given the finite amount of data available, a decision maker would find it difficult statistically to distinguish members of a set of alternative models located inside the entropy ball. Detection-error probabilities can be calculated using likelihood ratio tests given a fixed sample of observations. Since the damage function used in the climate models are basically calibrated functions not estimated from actual date we did not calculate detection probabilities. Instead we focused in calculating the impact on the paths of the variables of interest, that is, emissions, cumulative emissions, temperature anomaly and carbon taxes from increasing the robustness parameters relatively to the benchmark case.[11]

The four scenarios were run with and without an effective temperature constraint. The unconstrained case results in temperature anomaly paths which exceed the 1.5°C threshold before the end of the 100 year time horizon, while in the constrained case the anomaly paths never exceed the threshold. In the simulations the threshold is set at 0.5°C since the current anomaly relative to the pre-industrial period is approximately 1°C.

The constrained and unconstrained programs were solved for a pre- and a post-pandemic scenario aiming at exploring the impact of the pandemic on climate change (Figures 2-5). For the post-pandemic case we run an optimistic and a pessimistic scenario. In the optimistic scenario we expect the 99% recovery to require two years, while in the pessimistic scenario it requires four years. Here we report the results of the pessimistic scenario only, since the pessimistic pandemic is "optimistic" for climate change, in the sense that emissions are reduced for a longer time and we want to explore the impact of the pandemic on temperature under a scenario which is the most "favorable" for climate.

Each scenario produced as outputs: (i) the optimal path of CO_2 emis-

[10] See also Hansen Sargent and Wang (2002) or Dennis et al. (2004).

[11] In principle detection probabilities could have been calculated for the temperature anomaly for which data exist. We choose to have a uniform approach for dealing with the robustness parameters.

sions, (ii) the corresponding cumulative CO_2 emissions path, (iii) the path for the temperature anomaly resulting under the temperature dynamics and the cumulative emission paths, and (iv) the optimal path for the carbon tax.

Figure 2 shows the solutions of the unconstrained problem for the pre-pandemic case. We observe that annual emissions decrease monotonically as we shift from scenario 1 to scenario 4, that is, as new risk factors and larger misspecification concerns add up. This result is consistent with Rudik's (2020) finding that *"the misspecification insurance channel"* reduces emissions. The 1.5°C temperature target will be surpassed in approximately 65 years from now in scenario 1, in 70 years in scenario 2, in 75 years in scenario 3 and in 100 years in scenario 4. Thus misspecification concerns make the attainment of the temperature target easier. Figure 3 shows the solutions of the constrained problem for the pre-pandemic case. Annual emissions have to be reduced more drastically relative to the unconstrained case over the 100-year horizon if the constraint is to be satisfied. We observe that higher misspecification concerns in damages require a higher reduction of emissions at the beginning (compare scenarios 4 and 3), but the trajectories of emissions show crossing effects around 45 years from now.

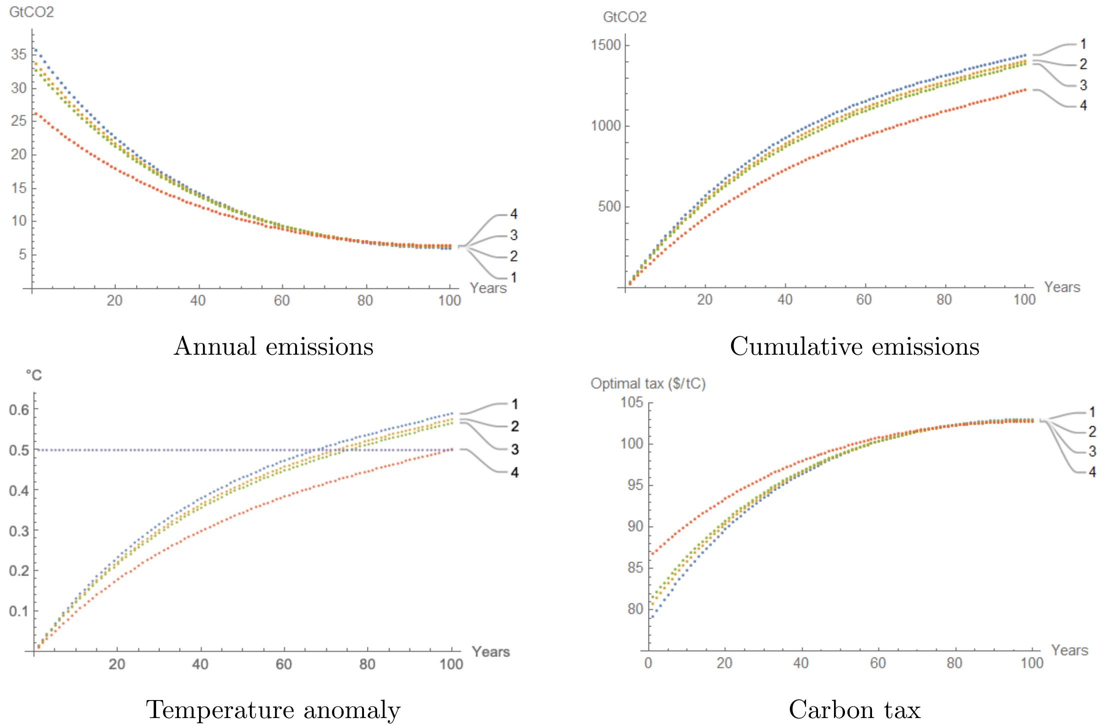

Figure 2. Unconstrained pre-pandemic optimal paths

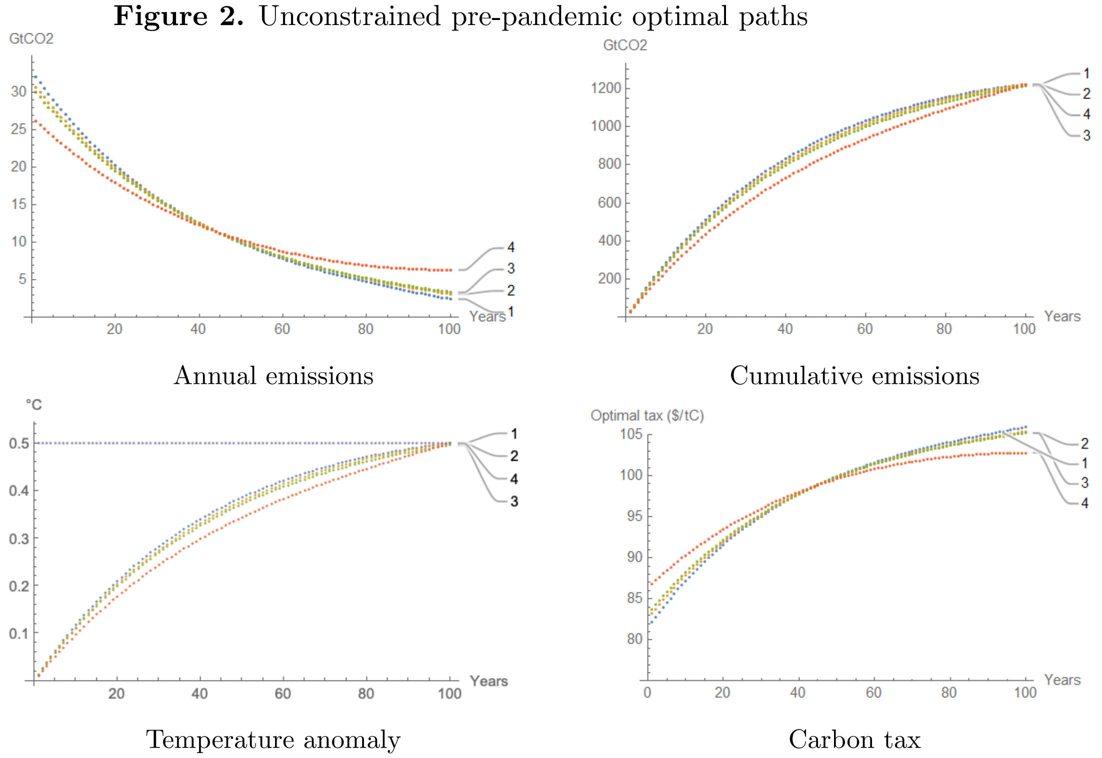

Figure 3. Constrained pre-pandemic optimal paths

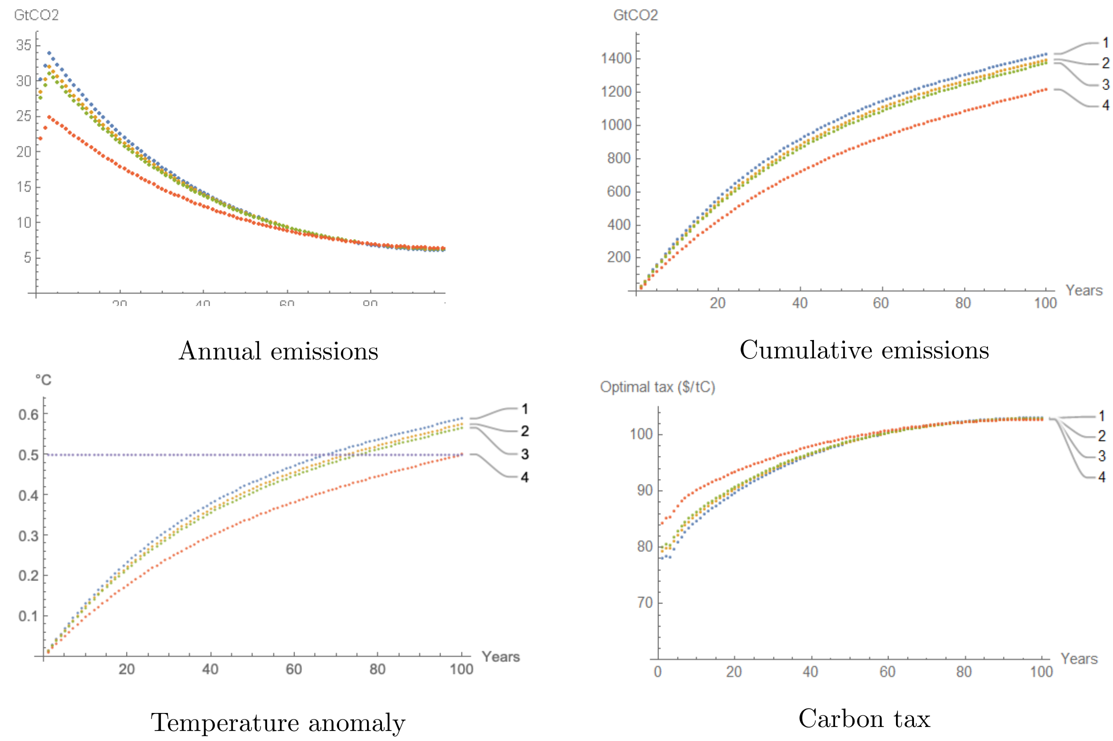

Figure 4. Post-pandemic unconstrained optimal paths

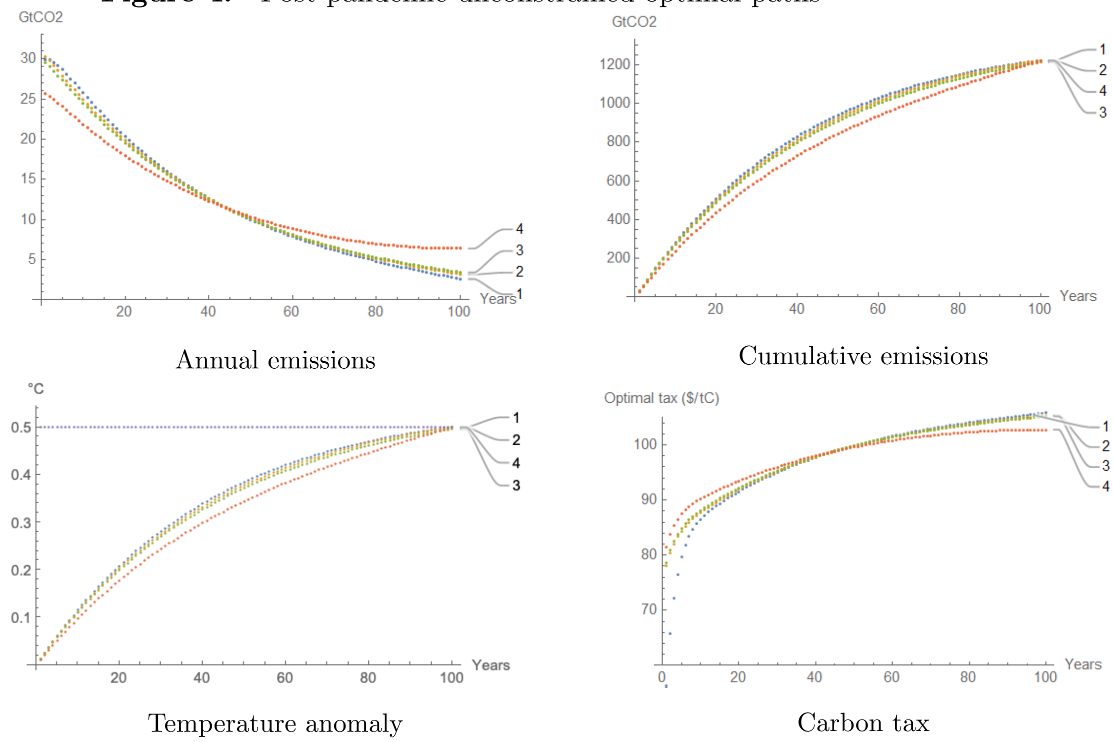

Figure 5. Post-pandemic constrained optimal paths

The intuition is that strong misspecification concerns lead to strong action in terms of higher emission reduction relative to the risk cases (scenarios 1 and 2). Once the concerns have been satisfied in the first half of the horizon, the policy becomes more relaxed. This is more profound in the constrained case (Figure 3) when strong action is taken so that once the economy is *"locked"* on a path which could satisfy the constraint under the worst case scenario, emissions can be increased relative to the no concerns case later on. In a sense deep uncertainty calls for strong actions now, however the strong action in terms of emission reductions now is compensated by weaker action in the future. The addition of jumps does not change the qualitative results significantly, although it decreases further emissions in comparison to scenario 1.

We compute the optimal carbon taxes using expression (12). The paths of the optimal carbon taxes, consistent with unconstrained emissions in Figure 2 and constrained emissions in Figure 3, are increasing in time. The range of values of the carbon taxes we found is about \$78-87/tC as initial taxes in the unconstrained case and about \$82-87/tC in the constrained case, up to \$102/tC in 100 years for the former case and \$100-104/tC for the latter. Starting optimal taxes in these intervals seems to be in line with the recommendations of the High-Level Commission on Carbon Prices (2017). Our results – that optimal carbon taxes increase along the path, but at a decreasing rate and, at the same time, constrained carbon emissions are strictly decreasing over time, but at a decreasing rate – are consistent with the results in Dietz and Venmans (2018), even though they develop a deterministic model.[12]

Comparison of scenarios 3 and 4 in the constrained case shows that a higher misspecification concern results in a higher carbon tax initially (\$87/tC in scenario 4 and \$84/tC in scenario 3) relative to the pure risk case. Around 45 years from the initial time, path-crossing occurs and taxes under the strongest concerns become the lowest even as compared to the no-concerns cases (scenarios 1 and 2). Eventually, the carbon tax is ramped up to \$100/tC in scenario 4 and \$103/tC in scenario 3. A policy of high taxes caused by deep uncertainty early on is compensated by a lower tax

[12] They actually find that the optimal carbon price under a temperature constraint equals the social cost of carbon plus a premium, which is a function of the cumulative emissions constraint and increases at the discount rate. Rezai and van der Ploeg (2016) and van der Ploeg (2018) obtain a similar result.

policy later on. This result, that the optimal carbon tax trajectories can cross when different uncertainty channels are considered, can also be found in Rudik (2020), although he does not distinguish between constrained and unconstrained cases.

The introduction of the pandemic shock in both the constrained and the unconstrained problem causes emissions to decrease significantly at the beginning as a result of the containment and lockdown measures (Figures 4 and 5), but the overall results are qualitatively similar to the pre-pandemic case. The emission reduction is short-lived, with a post-crisis rebound that restores emissions close to their original trajectory. This preliminary analysis suggests that the COVID-19 pandemic will have negligible effects on the evolution of the temperature anomaly.

Sensitivity analyses on the other parameters, for example, ρ, ε and Γ, where the base case uses the parameter values of the scenarios above, is possible. It shows (not reported here for brevity) that the optimal annual emissions are larger if the parameter ρ is higher than zero; that is, if the damage impact of emissions weakens with the passage of time, then more emissions are allowed on the optimal path and the corresponding emission tax is lower relative to the case $\rho = 0$, which corresponds to the case in which past emissions have the same damage effects as current emissions. The sensitivity of the solution is, however, very small, in the neighborhood of $\rho = 0$.[13] Furthermore, an increase in ε (the impact of emissions on damages), in aversion to risk γ and/or volatility σ (which is embodied in parameter Γ), will cause a monotonic reduction in the optimal amount of annual emissions. In conclusion, concerns about risk and deep uncertainty lead to a more restrained policy by reducing emissions and increasing carbon taxes. An interesting policy result is that deep uncertainly calls for strong actions earlier which can be significantly relaxed later on.

6.1 The risk-adjusted interest rate

Even though our model does not include asset markets, we can compute the risk-adjusted interest rate in this context. It is expected that since the economy would be indifferent between emitting and paying a carbon tax

[13] This suggests that the case of $\rho = 0$, which corresponds to a quadratic damage function when the temperature anomaly is linear in cumulative emissions, could be regarded as a reasonable approximation.

the current period or the next period, carbon taxes should increase at the risk-adjusted interest rate. Figure 6 presents the rate of change of carbon taxes for scenario 3 under the effective temperature constraint.

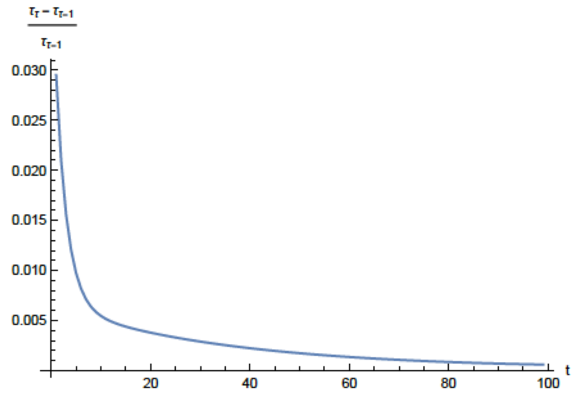

Figure 6: Carbon tax rate of growth

Figure 6 shows that the carbon price that ensures that temperature stays below the temperature cap grows first at a relatively high rate and then over time the growth rate of the carbon price tapers off. Figure 6 shows that the optimal carbon price growth rate decreases from 3% down to 0.5% in about 10 years for scenario 3. The initial value of 3% is broadly consistent with Olijslagers et al. (2021), which in a scenario with uncertainty, macro disasters shocks and a temperature cap, calibrated a real risk-free interest rate of 0.75% and a risk premium of 2.65%, implying that the optimal carbon price grows in expectation at a rate equal to 3.4%.

The decreasing shape of Figure 6 is also in accord with Gollier (2020), who found discount rates of about 4.14% for short horizons down to less than 1.6% for very long horizons. Our Figure 6 could be interpreted as the decreasing socially efficient discount rate as a function of the time horizon (Gollier, 2002).

Various theories have suggested a downward-sloping term structure for the interest rate (Gollier, 2020). Here the declining growth rate of the carbon price is mostly determined by misspecification concerns. We have computed the optimal carbon price growth in the absence of misspecification concerns, both for scenario 1 and scenario 2, and found that even though there is a slight downward-sloping shape in both cases, the spread is almost zero over time, confirming that this effect is mostly related to the robust control approach.

6.2 The cost of robustness

Using the same parametrization, we calculate the difference (15) for the post-COVID-19 case for the constrained and unconstrained problems[14] and compare the loss in welfare – as it is defined in our model – from adopting robust control methods, relative to the benchmark case of unconstrained no-misspecification concerns which corresponds to scenario 1. Since the benchmark model corresponds to the case of risk the results can be interpreted as the cost of precaution when temperature targets are introduced. The results are shown in Figure 7 for increasing robustness parameters θ and for three different values for the robustness parameter υ. The range of values for the robustness parameters was chosen such that at the end of the planned horizon the maximum misspecification concern will not lead to a temperature path which will overshoot the target anomaly of 0.5°C by 0.15°C.[15] This means that the regulator is not willing to accept misspecification concerns that will lead to a reduction of emissions such that the anomaly will be 0.35°C, instead of 0.5°C at the end of the planning horizon. As shown in Figure 7 this discipline of the robustness parameters implies that the regulator is not willing to accept losses in welfare relative to the benchmark model due to precautionary behavior in the range of 90%.

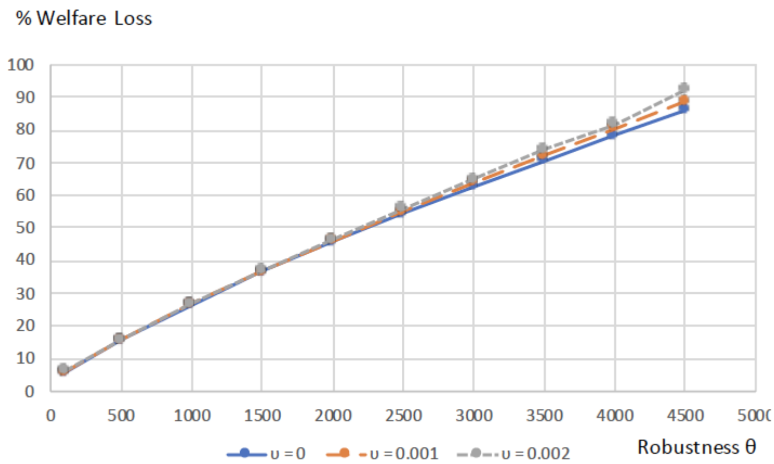

[14]The Mathematica code for calculation of the sum (14) can be found in the supplementary material.

[15]This implies the distance function

$$\rho_0\left(0.5, Y_k^R\right) = \max\left\{\left|0.5 - Y_k^R\right|; 1 \leq k \leq 100\right\}$$

with the constraint $\rho_0\left(0.5, Y_k^R\right) \leq 0.15$, for all k.

Figure 7: Welfare losses (%) due to robustness relative to the benchmark case.

Scenarios 3 and 4 correspond to $(\theta, \upsilon) = \{(100, 0.01), (1000, 0.02)\}$ respectively and there is no overshooting of the target. Misspecification concerns that lead to approximately 60% welfare losses overshoot the target by 0.09°C. In Figure 7 the line corresponding to $\upsilon = 0$ represents losses due to robustness preferences for damages only. When robustness preferences for temperature dynamics are added there a very small increase in losses. This suggest the robustness preferences for damages dominates welfare losses.

7 Concluding remarks

We develop a low-dimension analytic IAM with a holistic representation of uncertainty including traditional risk, described by a jump-diffusion process; "deep" uncertainty or misspecification concerns (which affect the evolution of temperature and of damages); and stochastic arrival of climate-related disasters. We derive and compare the optimal emission paths and carbon taxes between the constrained case where the global average temperature will not exceed the 1.5°C target and the unconstrained case. We provide analytic solutions and numerical results for a time horizon of 100 years.

In the context of our calibration, the estimated carbon budget consistent with the 1.5°C target is likely to be exhausted in less than 70 years with optimal – in the sense of the planner's optimality – but unconstrained emissions paths. Constrained emission paths are lower and carbon taxes are higher relative to the unconstrained case. When concerns about model misspecification and deep uncertainty increase, climate policy is more stringent in terms of lower emissions and high taxes relative to traditional risk in approximately the first half of the planning horizon, but the stringency is reversed in the second half. This result, given the strong uncertainties associated with climate change, supports the policy of "take strong action now". Precautious and robust control policy under deep uncertainty and misspecification concerns is costly in terms of our welfare indicator. Finally, preliminary investigation of the COVID-19 shock shows that the sharp emission reduction in the first half of 2020 seems to have been short-lived and will have a negligible effect on the evolution of the temperature anomaly. This suggests that green national programmes and international cooperation to mitigate climate should not be sidetracked by the pandemic.

8 Appendix

8.1 Appendix 1. Proof of Proposition 1

From the first-order conditions of (9) with respect to x_k, η_k and h_k, we obtain for $k = 1, ..., N$:

$$\delta^k \left\{ u - D_0 - [(\varepsilon + w + \Gamma k)x_k + \varepsilon \sum_{j=1}^{k-1} \beta^{k-j} x_j + \Gamma \sum_{i<k} i x_i + \sigma_0 \eta_k] \right\} - \lambda\Lambda = 0 \tag{18}$$

$$\delta^k \left(-\sigma_0 x_k + \frac{\eta_k}{\theta} \right) = 0 \tag{19}$$

$$\delta^k \frac{h_k}{v} - \lambda \sigma_m = 0, \tag{20}$$

where $\lambda \geq 0$ is a Lagrange multiplier, yielding $\eta_k = \sigma_0 \theta x_k$ and $h_k = \lambda \sigma_m v \delta^{-k}$ (from (19) and (20)). Notice that $\eta = 0$ if σ_0 or $\theta = 0$, and $h_k = 0$ if σ_m or $v = 0$. Plugging η_k and h_k into (18), we get the optimal solutions for x_k. This amounts to solving a linear system as in (10) in the text. Moreover, since the constraint can be written as $\Lambda \Xi^T \mathbf{x}^* = \alpha - A\lambda$, where Ξ is a vector with all entries equal to 1, and $A = \sigma_m^2 v \sum_i \delta^{-i}, i = 1, ..., N$, after replacing h_k from (20) we get:

$$\begin{aligned} \Lambda \Xi^T \mathbf{x}^* &= \alpha - A\lambda = \Xi^T M^{-1} \Xi \Lambda (u - D_0) - \lambda \Lambda^2 \Xi^T M^{-1} \begin{pmatrix} \delta^{-1} \\ ... \\ \delta^{-N} \end{pmatrix} \\ \lambda &= \frac{(u - D_0)\Lambda \sum_{i,j} \widetilde{m}_{i,j} - \alpha}{\Lambda^2 \sum_{i,j} \widetilde{m}_{i,j} \delta^{-j} - A}, \text{ with } M^{-1} = (\widetilde{m}_{i,j}). \end{aligned}$$

For example, if $N = 1$, $v = \theta = 0$, then $\lambda = \frac{\delta}{\Lambda}(u - D_0) - \frac{\alpha\delta}{\Lambda^2}(\varepsilon + w + \Gamma)$.

8.2 Appendix 2. Extension to climate-related disasters

Let us consider the case of climate-related disasters as described in Section 4. Following the same procedure as in Section 3, we can write the Lagrangian associated with the corresponding robust control problem as:

$$\sum_{k=1}^{N} \delta^k \left\{ (u - D_0)x_k - \left(q_0 + \xi \left(\Lambda \sum_{j=1}^{k-1} x_j + \sum_{j=1}^{k-1} \sigma_m h_j\right)\right) \zeta(a + bx_k) - [(\varepsilon + w + \Gamma k)\frac{x_k^2}{2} + \varepsilon x_k \sum_{j=1}^{k-1} \beta^{k-j} x_j + \Gamma x_k \sum_{i<k} i x_i + \sigma_0 \eta_k x_k] - \frac{\gamma}{2}\left(q_0 + \xi \left(\Lambda \sum_{j=1}^{k-1} x_j + \sum_{j=1}^{k-1} \sigma_m h_j\right)\right) \zeta^2 (a + bx_k)^2 + \frac{\eta_k^2}{2\theta} + \frac{h_k^2}{2\upsilon} \right\} - \lambda \left[\Lambda \sum_{k=1}^{N} x_k + \sum_{k=1}^{N} \sigma_m h_k - \alpha\right], \tag{21}$$

which differs from the expression obtained in Section 3 because of the changes in the expectation of damage and of the variance term, which is:

$$\mathbb{E}_0[\sigma^2(\sum_{k=1}^{N} x_k W_k)^2] + \mathrm{var}_0[J_N] =$$
$$\sigma^2 \sum_{k=1}^{N} [x_k^2 k + 2x_k \sum_{i<k} i x_i] +$$
$$\sum_{k=1}^{N} (q_0 + \xi(\Lambda \sum_{j=1}^{k-1} x_j + \sum_{j=1}^{k-1} \sigma_m h_j))\zeta^2 (a + bx_k)^2.$$

Computing the first-order conditions with respect to x_k, η_k and h_k, we get equations of the second order in x, which have to be solved numerically. However, for small ζ we can neglect the term ζ^2 and thus we can determine the optimal emission policy by solving a linear system of the form:

$$\widehat{M} \begin{pmatrix} x_1 \\ x_2 \\ \dots \\ x_N \end{pmatrix} = \begin{pmatrix} (u - D_0 - q_0\zeta b - \lambda\Lambda\delta^{-1}) \\ (u - D_0 - q_0\zeta b - \xi\zeta b\lambda\upsilon\sigma_m^2\delta^{-1} - \lambda\Lambda\delta^{-2}) \\ \dots \\ (u - D_0 - q_0\zeta b - \xi\zeta b\lambda\upsilon\sigma_m^2 \sum_{i=1}^{N-1}\delta^{-i} - \lambda\Lambda\delta^{-N}) \end{pmatrix},$$

where the matrix $\widehat{M}$ is:

$$\widehat{M} = \begin{pmatrix} (\varepsilon + w + \Gamma + \sigma_o^2\theta) & (\varepsilon\beta + \Gamma + \xi\zeta b\Lambda) & \dots & (\varepsilon\beta^{N-1} + \Gamma + \xi\zeta b\Lambda) \\ (\varepsilon\beta + \Gamma + \xi\zeta b\Lambda) & (\varepsilon + w + 2\Gamma + \sigma_o^2\theta) & \dots & (\varepsilon\beta^{N-2} + 2\Gamma + \xi\zeta b\Lambda) \\ \dots & & & \dots \\ (\varepsilon\beta^{N-1} + \Gamma + \xi\zeta b\Lambda) & (\varepsilon\beta^{N-2} + 2\Gamma + \xi\zeta b\Lambda) & \dots & (\varepsilon + w + N\Gamma + \sigma_o^2\theta) \end{pmatrix}$$

and

$$\lambda = \frac{(u-D_0)\Lambda\sum_{i,j}\widehat{m}_{i,j}-\alpha}{\Lambda^2\sum_{i,j}\widehat{m}_{i,j}\delta^{-j}-A}$$

$$\text{with } A = \sigma_m^2 v\sum_i \delta^{-i} \text{ and } \widehat{M}^{-1}=(\widehat{m}_{i,j}).$$

The above expressions lead to an extension of Proposition 1 when the risk of extreme events is included. Thus, the optimal emission policy is obtained as:

$$\mathbf{x}^* = \begin{pmatrix} x*_1 \\ x*_2 \\ ... \\ x*_N \end{pmatrix} = \widehat{M}^{-1}\begin{pmatrix} (u-D_0-q_0\zeta b-\lambda\Lambda\delta^{-1}) \\ (u-D_0-q_0\zeta b-\xi\zeta b\lambda v\sigma_m^2\delta^{-1}-\lambda\Lambda\delta^{-2}) \\ ... \\ (u-D_0-q_0\zeta b-\xi\zeta b\lambda v\sigma_m^2\sum_{i=1}^{N-1}\delta^{-i}-\lambda\Lambda\delta^{-N}) \end{pmatrix}.$$

8.3 Appendix 3. Calibration

The damage function

We use Nordhaus's DICE 2016R calibration in which damage as a proportion of gross GDP is given by

$$D = 0.00236\,(\Delta T)^2\,,$$

where ΔT is increase in temperature of the atmosphere (in degrees C from 1900). We calculate world GDP in year 2018 in 2011 US international \$ at 119.530×10^{12} (in 2011 US international \$), from world GDP per capita at \$15,914 and world population at 7.511 billion.[16] By considering that since the pre-industrial period, average global temperature has increased by approximately 1°C temperature (IPCC, 2018), then (2) implies for the deterministic part of damages that:

$$0.00236\times119.530\times10^{12.} = \varepsilon\left[\sum_{j=1}^{k}\left(\frac{x_j^2}{2}+\sum_{i<j}e^{-\rho(j-i)}x_ix_j\right)\right].$$

Using CO_2 emissions in 1751 (initial period) and CO_2 emissions in 2018 (i.e., k), we calculate the term in brackets ($4.13578\times10^{17}(CO_2)^2$) which results

[16] See World Bank https://data.worldbank.org/indicator/NY.GDP.PCAP.PP.KD

in $\varepsilon = 2.82 \times 10^{-6}$.

Damages from the stochastic arrival of climate disasters are assumed to be proportional to a linear approximation of the quadratic benefit function at the level of 36 $GtCO_2$ which is regarded as the current pre-pandemic level of annual emissions. The slope of the linear approximation is billion $\$/GtCO_2$.

The benefit function

We use a quadratic benefit function of the form

$$U_k = U_0 + ux_k - \frac{1}{2}wx_k^2 \ , k = 1, 2, \dots \ .$$

In calibrating the parameters u and w, which are the relevant parameters for the optimization, we follow the procedure in Karp and Wang (2006). We revise the procedure so that the slopes of abatement cost are similar to those used by Nordhaus in DICE-2016R (September 2016). The abatement cost function was calibrated for the world GDP of 2018 as

$$A = 0.0943069v^{2.6} \times 119.53, \tag{22}$$

where v is the proportional reduction in CO_2 emissions relative to a business as usual scenario and 119.530×10^{12} is world GDP (in 2011 US international \$). Following Karp and Wang (2006), the quadratic benefit-of-emission function is equivalent to a quadratic abatement cost function

$$A = \frac{w}{2}\left(\bar{x} - x_k\right)^2 = \frac{w}{2}v\bar{x}.$$

As in Karp and Wang (2006), we draw 1,000 realizations of u from a uniform distribution with support $[0, 1]$, to allow for a carbon free world, and calculate A using (22); we treat the pairs (u, A) as psuedo-observations for a regression. The estimated $w = 2.95$ with $R^2 = 0.988$. The intercept is set at $u = 107.9$ which corresponds to zero abatement at the level of 36.572 $GtCO_2$.

In order to calibrate β, we follow the argument in Golosov *et al.* (2014) for the parameter describing the total fraction of a unit emitted at time 0 that is left in the atmosphere at time s. Such calibration is used by Rezai and van der Ploeg (2016). Their representation of the carbon cycle specifies the following parameters: (i) a share, φ_L, of carbon emitted into the atmosphere stays there forever; (ii) another share, $1 - \varphi_0$, of the remainder exits the atmosphere into the biosphere and the surface oceans; and (iii) a remaining part, $(1-\varphi_L)\varphi_0$, decays (slowly) at a geometric rate φ. Thus, the total fraction of a unit emitted at time 0 that is left in the atmosphere at time s equals $z_s = \varphi_L + (1-\varphi_L)\varphi_0(1-\varphi)^s$. We employ an annual time grid as in Rezai and van der Ploeg (2016) and suppose, as in Golosov *et al.* (2014), that after three decades half of the carbon has left the atmosphere, so that $z_{30} = 0.5$, a fifth of carbon stays up in the atmosphere forever ($\varphi_L = 0.2$), and the excess carbon that does not stay in the atmosphere "forever" has a mean lifetime of about 300 years ($(1-\varphi)^{300} = 0.5$, yielding $\varphi = .0.0231$). Therefore, $z_{30} = 0.5 = 0.2 + 0.8\varphi_0(1-0.0231)^{30}$ yielding $\varphi_0 = 0.402$. Thus, the value of β that minimizes the least square error between Golosov *et al.*'s (2014) formula and β^s is $\beta = 0.9546$.

As for the risk aversion parameter, we take $\gamma = 2$, which is consistent with the literature that usually takes values between 1 and 3 (see Pindyck, 2013). Finally, $\overline{\Phi}$ and H are calibrated as already explained in Section 5. The relevant parameter values are shown in Table A1.

Table A1. Parameter values

ε	2.82×10^{-6}		θ	0, 100, 1000*	
u	107.9	billion $\$/GtCO_2$	v	0, 0.001, 0.0001*	
w	2.95	billion $\$/(GtCO_2)^2$	ξ	0.0128**	
δ	$1/(1+0.01)$		ζ	0.01	
γ	2		b	4.65	billion $\$/GtCO_2$
σ	0.03		$\overline{\Phi}$	0.9	
Λ	0.00040905	$°C/GtCO_2$	H	0.52	
σ_0	0.03		$\bar{R}$	4	Pessimistic recovery
σ_m	0.01				

* For scenarios 1(benchmark), 3 and 4.

** Karydas and Xepapadeas (2020).

References

Anderson, E. W., Brock, W., Hansen, L. P., and Sanstad, A. H. (2014), Robust analytical and computational explorations of coupled economic-climate models with carbon-climate response, RDCEP WP 13-05.

Anderson, E.w., Hansen, L.P. and Sargent, T.J. (2003), "A quartet of semigroups for model specification, robustness, prices of risk, and model detection," Journal of the European Economic Association 1 (1), 68–123.

Anderson, E. W., Hansen, L. P., and Sargent, T. J. (2012), Small noise methods for risk sensitive/robust economies, *Journal of Economic Dynamics and Control 36*, 468–500.

Anthoff, D. and Tol, R. (2013), The uncertainty about the social cost of carbon: A decomposition analysis using fund, *Climate Change 117*, 515–530.

Barnett, M., Brock. W. A., and Hansen, L. P. (2020), Pricing uncertainty induced by climate change, *The Review of Financial Studies 33*, 1024–1066.

Barnett, M., Brock. W. A., and Hansen, L. P. (2021) Climate Change Uncertainty Spillover in the Macroeconomy, Available at:
https://larspeterhansen.org/research/papers/

Barro, R. (2009), Rare disasters, asset prices, and welfare costs, *American Economic Review 99*, 243–64.

Brock, W. A. and Carpenter S. R. (2006), Rising variance: A leading indicator of ecological transition, *Ecology Letters 9*, 311–318.

Burke, M., Hsiang, S. M., and Miguel, E. (2015), Global non-linear effect of temperature on economic production, *Nature 527*, 235–239.

Cai, Y. and Lontzek, T. S. (2019), The Social Cost of Carbon with Economic and Climate Risk, *Journal of Political Economy 127*, 2684–2734.

Campi, M. C. and James, R. M. (1996),Non-linear discrete time risk-sensitive optimal control, *International Journal of Robust and nonlinear Control 6*, 1-19.

Cerreia-Vioglio S, Maccheroni F, Marinacci M, Montrucchio L (2011) Uncertainty averse preferences. *Journal of Economic Theory* 146(4):
1275–1330.

Dennis, R., Leitemo, K, and U. Söderström, (2004), Methods for Robust Control, CEPR, Discussion Paper No. 5638

Dietz, S., Bowen, A., Doda, B., Gambhir, A., and Warren, R. (2018), The economics of 1.5°C climate change, *Annual Review of Environment and*

Resources, 43, 455–480.

Dietz, S. and Venmans, F. (2019), Cumulative carbon emissions and economic policy: In search of general principles, *Journal of Environmental Economics and Management 96*, 108–129.

Dockner, E. J. and Van Long, N. (1993), International pollution control: Cooperative versus noncooperative strategies, *Journal of Environmental Economics and Management 25*, 13–29.

European Commission (2019), The European Green Deal, Communication COM(2019) 640 final, available at https://eur-lex.europa.eu/legal-content/EN/ALL/?uri=CELEX:52019DC0640

Fitzpatrick, L.G. and Kelly, D.L. (2017) Probabilistic Stabilization Targets, *Journal of the Association of Environmental and Resource Economists,4, 611-657*

Gerlagh, R. and Liski, M. (2016) Carbon prices for the next hundred years, *The Economic Journal 128*, 728–757.

Gilboa I, Schmeidler D (1989) Maxmin expected utility with nonunique prior. *Journal of Mathematical Economics* 18(2):141–153.

Gillingham, K., Nordhaus, W., Anthoff, D., Bosetti, V., McJeon, H., Blanford, G. J., Christense, P., Reilly, J. M, and Sztorc, P. (2016), Modeling uncertainty in climate change: a multi-model comparison, FEEM, WP013-2016.

Gollier, C (2002), Discounting an uncertain future, *Journal of Public Economics,* 85, 149-166

Gollier, C (2020), The cost efficiency carbon pricing puzzle, Toulouse University

Golosov, M., Hassler, J., Krusell, P., and Tsyvinski, A. (2014), Optimal taxes on fossil fuel in general equilibrium, *Econometrica 82*, 41–88.

Hansen, L. P. and Sargent, T. J. (2001), Robust control and model uncertainty, *The American Economic Review 91*, 60–66.

Hansen, L. P., Sargent, T. J., and N. Wang (2002), Robust permanent income and pricing with filtering, Macroeconomic Dynamics 6 (1), 40–84.

Hansen, L. P. and Sargent, T. J. (2003), Robust control of forward-looking models, *Journal of Monetary Economics* 50, 581–604

Hansen, L. P., Sargent, T. J., Turmuhambetova, G. and Williams, N. (2006), Robust control and model misspecification, *Journal of Economic Theory 128*, 45–90.

Hansen, L. P. and Sargent, T. J. (2008), *Robustness,* Princeton University Press.

Hassler, J., Krusell, P., and Olovsson, C. (2018), The consequences of uncertainty climate sensitivity and economic sensitivity to the climate, *Annual Review of Economics 10*, 189–205.

Heal, G. and Millner, A. (2014), Uncertainty and decision-making in climate change economics, *Review of Environmental Economics and Policy 8*, 1, 120–137.

High-Level Commission on Carbon Prices (2017) Report of the High-Level Commission on Carbon Prices. World Bank, Washington, DC.

IEA (2020), *Global Energy Review 2020*, International Energy Agency, Paris.

IMF (2020), *World Economic Outlook: A Long and Difficult Ascent*, International Monetary Fund, Washington, DC.

IPCC (2014), *Climate Change 2014. Synthesis Report, Summary for Policymakers*, Contribution of Working Groups I, II and III to the Fifth Assessment Report of the Intergovernmental Panel on Climate Change, Core Writing Team, Pachauri R.K. and L.A. Meyer (eds), IPCC, Geneva, Switzerland.

IPCC (2018) Special Report, Global Warming of 1.5 °C, available at https://www.ipcc.ch/report/sr15/.

Karp, L. S. and Zhang, J. (2006), Regulation with anticipated learning about environmental damages, *Journal of Environmental Economics and Management 51*, 259–279.

Karydas, C. and Xepapadeas, A. (2019), Pricing climate change risks: CAPM with rare disasters and stochastic probabilities, Mimeo.

Klibanoff P, Marinacci M, Mukerji S (2005) A smooth model of decision making under ambiguity. *Econometrica* 73(6):1849–1892

Knutti, R., Joos, F., Muller, S. A., Plattner, G.-K., and Stocker, T. F. (2005), Probabilistic climate change projections for CO_2 stabilization profiles, *Geophysical Research Letters 32*, doi:10.1029/2005GL023294.

Lemoine, D. (2010), Paleoclimatic warming increased carbon dioxide concentrations, *Journal of Geophysical Research 115*, D22122.

Le Quere, C., Jackson, R. B., Jones, M. W., Smith, A. J. P., Abernethy, S. *et al.* (2020), Temporary reduction in daily global CO_2 emissions during the COVID-19 forced confinement, *Nature Climate Change 10*, 647–653.

Maccheroni F, Marinacci M, Rustichini A (2006) Ambiguity aversion, robustness, and the variational representation of preferences. *Econometrica* 74(6):1447–1498.

Manoussi, V., Xepapadeas, A., and Emmerling, J. (2018), Climate emgineering under deep uncertainty, *Journal of Economic Dynamics and Control 94*, 207–224.

Matthews, H. D., Gillett, N. P., Stott, P.A., and Zickfeld, Z. (2009), The proportionality of global warming to cumulative carbon emissions, *Nature 459*, 829–833.

Matthews, H. D., Landry, J.-S., Partanen, A.-I., Allen, M., Eby, M., Forster, P. M., Friedlingstein, P., and Zickfield, K. (2017), Estimating carbon budgets for ambitious climate targets, *Current Climate Change Reports 3*, 69–77.

Matthews, H. D., Solomon, S., and Pierrehumbert, R. (2012), Cumulative carbon as a policy framework for achieving climate stabilization, *Philosophical Transactions of the Royal Society of London A 370*, 4365–4379.

Meinshausen, M., Meinshausen, N., Hare, W., Raper, S. C. B., Frieler, K., Knutti, R., and Allen, M. (2009), Greenhouse gas emission targets for limiting global warming to 2°C, *Nature 458*, 1158–1163.

Mengis, N., Partanen, A.-I., Jalbert, J., and Matthews, H. D. (2018), 1.5°C carbon budget dependent on carbon cycle uncertainty and future non-CO_2 forcing, *Scientific Reports 8*, article 5831, DOI:10.1038/s41598-018-24241-1.

Nordhaus, W. D. (1982) How Fast Should We Graze the Global Commons? *American Economic Review*, 72, 2, 242-46

Nordhaus, W. D. (2007), To tax or not to tax: the case for a carbon tax, *Review of Environmental Economics and Policy,* 1, 26-44

Nordhaus, W. D. and Moffat, A. (2017), A survey of global impacts of climate change: replication, survey methods and a statistical analysis. NBER WP. 23646, http://www.nber.org/papers/w23646.

Olijslager, S, van der Ploeg, F. and van Wijnbergen, S (2021), On current and future carbon prices in a risky world, Tinbergen Institute Paper No 21-045/VI

Petracou, E.V., Xepapadeas, A., Yannacopoulos, A.N. (2021) Decision making under model uncertainty: Fréchet–Wasserstein mean preferences. *Management Science,* https://doi.org/10.1287/mnsc.2021.3961

Pindyck, R. (2012), Uncertain outcomes and climate change policy, *Journal of Environmental Economics and Management*, 63, 289–303.

Pindyck, R. (2013), Climate change policy: What do the models tell us?, *Journal of Economic Literature*, 51, 3, 860–872.

Pindyck, R. (2017), The use and misuse of models of climate policy, *Review of Environmental Economics and Policy*, 11, 100-114

Rezai, A. and van der Ploeg, F. (2016), Intergenerational inequality aversion, growth and the role of damages: Occan's rule for the global carbon tax, *Journal of the Association of Environmental and Resource Economists*, 3, 2, 493–522.

Rudik, I. (2020), Optimal Climate Policy When Damages are Unknown, *American Economic Journal: Economic Policy*, 12, 2, 340-73

Solomon, S., Daniel, J. S., Sanford, T. J., Murphy, D. M., Plattner, G.-K., Knutti, R., and Friedlingstein, P. (2010), Persistence of climate changes due to a range of GHGs, *PNAS 107*, 18354–18359.

Tol, R.S.J (2013) Targets for Global Climate Policy, J*ournal of Economic Dynamics and Control,*37, 911-928

Traeger, C. (2015), Analytic integrated assessment and uncertainty, Mimeo, UC Berkeley, Available at http://www.lse.ac.uk/GranthamInstitute/wp-content/uploads/2015/04/Traeger_AnalyticIAM.pdf.

Traeger, C. (2018) ACE- Analytic Climatic Economy (with Temperature and Uncertainty), Available at https://papers.ssrn.com/abstract=3307622

van den Bijgaart, I., Gerlagh, R., and Liski, M. (2016), A simple formula for the social cost of carbon, *Journal of Environmental Economics and Management 77*, 75–94.

van den Bremer, T. and van der Ploeg, F. (2018), Pricing carbon under economic and climatic risk: Leading-order results from asymptotic analysis, OxCarre WP 203.

van der Ploeg, F. (2014), Abrupt positive feedback and the social cost of carbon, *European Economic Review 67*, 28–41.

van der Ploeg, F. (2018), The safe carbon budget, *Climatic Change 147*, 47–59.

Wachter, J. A. (2013), Can time-varying risk of rare disasters explain aggregate stock market volatility?, *The Journal of Finance 68*, 987–1035.

Weitzman, M. L. (2010), What is the *"damages function"* for global warming – and what difference might it make?, *Climate Change Economics*

1, 57–69.

Wigley, T. M. L. (2004), Choosing a stabilization target for CO_2, *Climate Change 67*, 1–11.

Supplementary Material

The Mathematica Code[17]

[17] The code was prepared by Petros Xepapadeas, Athens University of Economics and Business, p.xepapad@gmail.com.